



## Abstract

Ozone pollution represents a serious health and environmental problem. While ozone pollution is mostly produced by photochemistry in summer, elevated ozone concentrations can also be influenced by long range transport driven by the atmospheric circulation and stratospheric ozone intrusions. We analyze the role of large scale atmospheric circulation variability in the North Atlantic basin in determining surface ozone concentrations. Here, we show, using ground station measurements and a coupled atmosphere-chemistry model simulation for the period 1980–2005, that the North Atlantic Oscillation (NAO) does affect surface ozone concentrations – on average, over 10 ppbv on the monthly mean in southwestern, central and northern Europe – during all seasons except fall. The commonly used NAO index is able to capture the link existing between atmospheric dynamics and surface ozone concentrations in winter and spring but it fails in summer. We find that the first Principal Component, computed from the time variation of the sea level pressure (SLP) field, detects the atmosphere circulation/ozone relationship not only in winter and spring but also during summer, when the atmospheric circulation weakens and regional photochemical processes peak. The first Principal Component of the SLP field could be used as a tool to identify areas more exposed to forthcoming ozone pollution events. Finally, our results suggest that the increasing baseline ozone in western and northern Europe during the 1990s could be related to the prevailing phase of the NAO in that period.

## 1 Introduction

High ozone ( $O_3$ ) concentrations at the surface can have severe impact on human health and vegetation. In many of the modern cities and surrounding areas, ozone concentrations are often above the thresholds for plants damage and health effects especially during late spring and summer (e.g. Akimoto, 2003; Lövblad et al., 2004; Dentener et al., 2006; EEA report, 2010). Elevated  $O_3$  concentrations are local-to-regional phenomena, mainly associated with photochemical reactions favored by a combination of

ACPD

12, 3131–3167, 2012

## Model analysis and measurements intercomparison

F. S. R. Pausata et al.

Title Page

Abstract

Introduction

Conclusions

References

Tables

Figures

◀

▶

◀

▶

Back

Close

Full Screen / Esc

Printer-friendly Version

Interactive Discussion



**Model analysis and  
measurements  
intercomparison**

F. S. R. Pausata et al.

Title Page

Abstract

Introduction

Conclusions

References

Tables

Figures

◀

▶

◀

▶

Back

Close

Full Screen / Esc

Printer-friendly Version

Interactive Discussion



intense solar radiation and emissions of air pollutants. However, in the last twenty years, several studies have shown that tropospheric ozone can be transported over long distances, affecting  $O_3$  concentrations at the surface (e.g. Parrish et al., 1993; Fehsenfeld et al., 1996; Li et al., 2002; Creilson et al., 2003). This long range  $O_3$  transport mainly occurs during perturbed weather conditions, which, however, are generally not associated with highest surface  $O_3$  concentrations during summer. Nevertheless, long range transport of  $O_3$  and its precursors across the Atlantic basin does affect the mean surface  $O_3$  concentrations over Europe (e.g. Bronnimann et al., 2000, 2002; Simmonds et al., 2004 Fiore 2006).

Another source for surface  $O_3$  is associated with transport of stratospheric air into the troposphere (STT). Various dynamical mechanisms are responsible for transport of  $O_3$  enriched stratospheric air into the troposphere (Stohl et al., 2003), such as tropopause folds, cutoff lows, convective overshoots. While it is often difficult to attribute surface ozone to specific STT events, STT is important for ozone budget climatology and long term trends of surface ozone, due to continuous chemical  $O_3$  cycling entering the troposphere from the stratosphere (Lelieveld and Dentener, 2000; Hocking et al., 2007).

Regional scale processes, long range transport across the Atlantic Ocean and STT events over Europe are influenced by the North Atlantic Oscillation (NAO). The simplest NAO definition is “the tendency for pressure to be low near Iceland in winter when it is high near the Azores” and vice versa (Walker and Bliss, 1932). The NAO refers to swings in the atmospheric pressure difference between these two centers of action and dictates climate variability from the eastern seaboard of the United States to Siberia and from the Arctic to the subtropical Atlantic. Therefore, the NAO plays an important role in determining intercontinental transport of air masses as well as affecting regional scale atmospheric processes.

A common measure of the NAO phase is the so-called NAO index (NAOI) that is determined by the strength and the location of the semi-permanent Icelandic low and Azores high pressure systems (Walker, 1924; Walker and Bliss, 1932). The NAOI

is commonly defined as the difference in the normalized sea level pressure (SLP) anomalies between either Lisbon, Portugal, or Ponte Delgada, Azores, and Stykkisholmur/Reykjavik, Iceland (Hurrell, 1995). During positive NAO phases the Icelandic low deepens and the Azores high strengthens increasing the SLP gradient and consequently enhancing the westerly flow as well as intercontinental transport of air masses. This leads to above-normal precipitation and mild temperature over northern Europe, and drier weather conditions in the Mediterranean area. The negative phase of the NAO is associated with a slackening of the westerlies and enhanced meridional (N-S) atmospheric mass exchange. The weather related to low NAO phases is characterized by drier conditions in northern Europe and above-normal precipitation in southern Europe.

The NAO is mainly regarded as a winter phenomenon, since winter months are dynamically the most active and present the largest SLP amplitude anomalies. However, Barnston and Livezey (1987) showed that the NAO has a year-round influence on weather conditions in Europe with pronounced seasonal variation in location of the high and low pressure centers, and strong climate anomalies can also be detected outside the winter season. This is particularly important for summer, when atmospheric variability influenced by the NAO can lead to severe droughts and heat waves as well as prolonged photochemical smog. However, the NAOI as defined before is not able to accurately capture this variability in summer, since station-based indices are fixed in space and therefore cannot account for the seasonal migration of the NAO centers of actions. An alternative definition of NAOI is based on the empirical orthogonal function (EOF) analysis of the SLP field: the NAOI can be identified as the leading eigenvector (the first Principal Component, PC1) computed from the time variation of the SLP field. The associated PC1 is used to evaluate the temporal evolution of the NAO in any season. The spatial pattern representing the NAO is given by the leading EOF (EOF1). The advantage of using EOF analysis of the SLP field is that the PC1 index provide a more accurate representation of the NAO pattern taking into account the shifting of the NAO centers of action throughout the year.

**Model analysis and measurements intercomparison**

F. S. R. Pausata et al.

Title Page

Abstract

Introduction

Conclusions

References

Tables

Figures

◀

▶

◀

▶

Back

Close

Full Screen / Esc

Printer-friendly Version

Interactive Discussion



Li et al. (2002), using a 5-yr simulation performed with a three dimensional global chemistry model, found that North American influence on surface O<sub>3</sub> at Mace Head (Ireland) is strongly correlated with the NAO, especially in spring. Creilson et al. (2003) have described the link between the NAO and the seasonal and regional distribution of tropospheric ozone calculated using the tropospheric ozone residual technique. They have found a strong correlation between NAO and tropospheric O<sub>3</sub> over western Europe in spring. Other studies have investigated the long range transport of pollutants and O<sub>3</sub> precursors across the Atlantic into Europe associated with the NAO, using a chemistry-transport model (Duncan and Bey, 2004) and into the Arctic using passive tracers (Eckhardt et al., 2003). Sprenger and Wernli (2003) have shown that the NAO, affecting the synoptic-scale and meso-scale processes (cut-off lows and jet positions), also influences the STT of O<sub>3</sub> enriched air.

Most studies have used the station-based NAOI (e.g. Li et al., 2002; Creilson et al., 2003) to evaluate the behavior of long range transport of O<sub>3</sub> or other pollutants across the Atlantic Ocean, showing a weak if any correlation in the summer months. On the other hand, few studies have used the EOF-based index (PC1) to investigate intercontinental transport of gases and pollutants (Christoudias et al., 2012) or ozone variability (Hess and Lamarque, 2007). Using the ECHAM/MESSy atmospheric chemistry model with idealized water insoluble and soluble tracers, Christoudias et al. (2012) have investigated the influence of the NAO on the atmospheric dispersion of pollution, focusing only in winter when NAOI and PC1 are actually strongly correlated (Wallace, 2000). Hess and Lamarque (2007) have used a chemistry transport model to analyze tropospheric ozone variability in February and March only over the entire Northern Hemisphere, i.e. examining the Arctic Oscillation rather than isolating the NAO influence over the North Atlantic basin (the NAO can be seen as a part of the Arctic Oscillation).

The objective of this study is extending the previous works on the relationship of NAO and ozone to all seasons, including the high ozone season. This is of particular importance, since some climate model predictions have shown a trend towards more frequent positive NAO phases in the next decades (Fyfe et al., 1999; Gillett et al., 2001;

**Model analysis and measurements intercomparison**

F. S. R. Pausata et al.

Title Page

Abstract

Introduction

Conclusions

References

Tables

Figures

◀

▶

◀

▶

Back

Close

Full Screen / Esc

Printer-friendly Version

Interactive Discussion



Kuzmina et al., 2005; Stephenson and Pavan, 2006). Therefore it is of high relevance to clearly understand the link between the NAO and O<sub>3</sub> concentrations throughout the year and especially in summer when surface O<sub>3</sub> concentrations can be dangerous for the environment and human health. Here we compare the conventional station-based and the alternative EOF-based NAO definition in all seasons. We study the NAO/O<sub>3</sub> relationship using O<sub>3</sub> concentrations from several ground stations spread over Europe and then we extend this analysis applying a coupled atmosphere-chemistry model in a hindcast setup for the years 1980–2005. The comparison between these two indexes – using a 26 yr model simulation rather than few years as done in several previous studies (e.g. Li et al., 2002; Duncan and Bey, 2004) – provides a better overview about the relationship between O<sub>3</sub> variability and atmospheric dynamics. It also allows us to understand whether taking into account the latitudinal shifting in the atmospheric circulation throughout the year can improve our ability to detect correlations between atmospheric dynamics and O<sub>3</sub> concentrations. Furthermore, we analyzed O<sub>3</sub> anomalies through the depth of the troposphere associated with the two NAO phases in order to infer potential stratospheric influence onto surface O<sub>3</sub> concentrations.

In Sect. 2 we describe the data and the model used in this study. We present the NAO/O<sub>3</sub> relationship and O<sub>3</sub> concentrations anomalies associated with the NAO phases in Sect. 3. We discuss the implications of our findings in Sect. 4. Conclusions are presented in Sect. 5.

## 2 Data and methods

In this study we selected a total of 17 stations from the 150 stations belonging to the European Monitoring and Evaluation Programme (EMEP, <http://www.emep.int/>) for which monthly mean O<sub>3</sub> concentrations are available between 1990 and 2005 (Table 1). We have chosen a subset of relatively unpolluted stations with sufficiently long timeseries. We have considered only the monthly O<sub>3</sub> anomalies, removing the monthly annual mean from each stations. Given the proximity of the two Swedish stations (Rørwik and

### Model analysis and measurements intercomparison

F. S. R. Pausata et al.

Title Page

Abstract

Introduction

Conclusions

References

Tables

Figures

◀

▶

◀

▶

Back

Close

Full Screen / Esc

Printer-friendly Version

Interactive Discussion



Råö, ~3 km) and the years available (1990–2002 and 2003–2005), we have merged their monthly O<sub>3</sub> anomalies timeseries.

In addition to the measurement data analysis, we have extended our study using the model results from the re-analysis simulation of Pozzoli et al. (2011). The chemical composition of the troposphere was simulated for the period 1980–2005 with the fully coupled aerosol-chemistry climate model, ECHAM5-HAMMOZ, described in detail in Pozzoli et al. (2008a). The model is composed of the general circulation model ECHAM5 (Roeckner et al., 2003, 2006; Hagemann et al., 2006), the tropospheric chemistry module MOZ (MOZART-2, Horowitz et al., 2003), and the aerosol module HAM (Stier et al., 2005). The meteorological fields and chemical composition of the troposphere are available at the horizontal resolution of about  $2.8 \times 2.8^\circ$ , and with 31 vertical levels from the surface up to 10 hPa. The meteorology was nudged (Jeuken et al., 1996) with the ECMWF ERA-40 re-analysis (Uppala et al., 2005) until 2000 and by operational analyses (IFS cycle-32r2) for the remaining period (2001–2005). We must note that this discontinuity may have an impact on the meteorological variables; however, Pozzoli et al. (2011) did not find any evidence for this. The nudging technique forces the large scale dynamic state of the atmosphere towards the re-analysis data, the model is in a consistent physical state at each time step but it calculates its own physics.

We used one of the two transient simulations performed in Pozzoli et al. (2011) (their SREF simulation), in which anthropogenic emissions are changing on an hourly-to-monthly basis (for more details refer to Pozzoli et al., 2011).

The ECHAM5-HAMMOZ model has been extensively evaluated in previous studies (Stier et al., 2005; Pozzoli et al., 2008a,b, 2011; Auvray et al., 2007; Rast et al., 2012) with comparisons to several measurements and within model intercomparison studies. We must remark a substantial overestimate of our computed ozone compared to measurements by up to 15 ppbv in some regions, a problem that ECHAM5-HAMMOZ shares with many other global models (Ellingsen et al., 2008). Nevertheless, the model captures the observed range of interannual O<sub>3</sub> variability. Pozzoli et al. (2011) analyzed

## Model analysis and measurements intercomparison

F. S. R. Pausata et al.

Title Page

Abstract

Introduction

Conclusions

References

Tables

Figures

◀

▶

◀

▶

Back

Close

Full Screen / Esc

Printer-friendly Version

Interactive Discussion



seasonally averaged modeled and measured surface ozone concentrations and found a reasonably well agreement for a large number of North American and European stations. The tropospheric O<sub>3</sub> burden (Stevenson et al., 2006) and variability (Hess and Mahowald, 2009) agree well with earlier studies.

The model data analyzed here are restricted to the Atlantic sector (20–90° N, 90° W–40° E) and the results are based on monthly anomalies from the climatological mean seasonal cycle. Standard Empirical Orthogonal Function (EOF)/Principal Component (PC) analysis has been used to calculate the leading mode of monthly SLP variability in the North Atlantic. The NAOI timeseries have been calculated as the difference in the normalized SLP anomalies between the model grid boxes corresponding to the location of Ponte Delgada, Azores and Stykkisholmur/Reykjavik, Iceland. The PC1 timeseries for each season has been normalized dividing it by its standard deviation. Hereafter we refer to NAO as the general term for the latitudinal shifting of air mass in all seasons not necessary linked to the station-based or PC1-based index (i.e. NAO = EOF1), whereas we clearly distinguish when we are referring to the PC1 or NAOI timeseries. The correlation between O<sub>3</sub> anomalies and NAOI/PC1 timeseries are calculated using the Pearson's linear correlation coefficient and all significant correlations discussed in the text refer to the 0.1 significance level (90 % confidence interval).

### 3 Results

The results presented here describe the correlations between the atmospheric variability and O<sub>3</sub> concentrations seen by ground station measurements and the atmosphere model. The results are presented in three sections. In the first section, we present the simulated climatological (1980–2005) SLP field and its variability, and tropospheric and surface O<sub>3</sub> mean state for each season. In the second section, we first discuss the general relationship between the NAOI/PC1 and the O<sub>3</sub> concentrations as measured by ground stations, and then we extend our analysis to the modeled NAOI/PC1 and O<sub>3</sub> relationship and the associated surface O<sub>3</sub> anomalies. In the third section, we

## Model analysis and measurements intercomparison

F. S. R. Pausata et al.

Title Page

Abstract

Introduction

Conclusions

References

Tables

Figures



Back

Close

Full Screen / Esc

Printer-friendly Version

Interactive Discussion



investigates O<sub>3</sub> anomalies through the depth of the troposphere, as represented by the model.

### 3.1 Simulated climatological (1980–2005) SLP and O<sub>3</sub> mean SLP climatology

The simulated SLP climatology, interannual variability and the NAO faithfully reproduce the observation (<http://www.cgd.ucar.edu/cas/jhurrell/indices.info.html#naostatann>), given that the simulated meteorology fields are relaxed towards the ERA-40 reanalyzed data. In the North Atlantic, the year-round SLP pattern is characterized by two main centers of action: a low and a high pressure systems situated in the proximity of Iceland and Azores respectively (Fig. 1), which determine the phase of the NAO – the dominant mode of atmospheric circulation in the Atlantic sector.

In winter, the NAO controls a significant fraction of the SLP variability in the North Atlantic accounting for more than 40 % of its total variance (Fig. 1). The SLP variability is also associated with pronounced atmospheric pressure swings between the positive and the negative phase of the NAO. Going towards summer, the amplitude of SLP swings and explained variability decreases reaching a minimum in summer (SLP swings are more than halved compared to winter) and fall (28 %) respectively. Considering the percentage of SLP variance explained in the different seasons, the maximum influence of the NAO on O<sub>3</sub> concentration is expected to be in winter, whereas the minimum in fall. The NAOI and PC1 monthly timeseries are strongly correlated in winter (0.86) when the atmospheric circulation is well described by the NAOI; whereas in summer, the correlation reaches the minimum (0.59), given the northward shift of the low and high pressure systems. In the transition seasons the PC1/NAOI correlation is around 0.75.

In the analyzed period, the PC1 timeseries shows a persistent NAO positive phase from 1988 till 1996 in all seasons, except in fall when no preferred phase is found (Fig. 1). This persistent NAO positive phase is particularly evident in winter when from 1988 to 2000 only the period 1996–1998 have shown a weak negative NAO phase.

## Model analysis and measurements intercomparison

F. S. R. Pausata et al.

Title Page

Abstract

Introduction

Conclusions

References

Tables

Figures

◀

▶

◀

▶

Back

Close

Full Screen / Esc

Printer-friendly Version

Interactive Discussion



## Tropospheric ozone mean climatology

In this section we compare model calculated tropospheric ozone average with satellite determined ozone, to verify the large-scale consistency of spatial and temporal patterns. To this end we use the tropospheric O<sub>3</sub> load inferred by using the Tropospheric Ozone Residual (TOR) technique (Fig. 3). The TOR technique uses measurements from the Total Ozone Mapping Spectrometer and Solar Back scattered Ultraviolet instruments and it is described in details in Fishman et al., 2003. Both the TOR values and the tropospheric O<sub>3</sub> burden in this study have being derived using the definition of the thermal tropopause, which it is determined when the lapse rate does not exceed 2 K km<sup>-1</sup> for 2 km above. Like surface ozone (Sect. 2), also the modeled tropospheric O<sub>3</sub> burden exhibits an overestimation compared to the satellite observations (Fig. 3).

The simulated surface (Fig. 2) and tropospheric O<sub>3</sub> (Fig. 3) shows a distinct seasonal cycle that peaks mostly in late spring/early summer and reaches a minimum in winter. The simulated tropospheric O<sub>3</sub> shows a remarkably similar behavior to the TOR values (Fig. 3). The small discrepancies in pattern could be attributed to the lower resolution of the climate model ( $\sim 3 \times 3^\circ$ ) compared to the TOR grid ( $\sim 1 \times 1^\circ$ ).

As mentioned in Sect. 2, for the scope of this paper the overestimation of the O<sub>3</sub> values does not represent an issue, since the focus of this study is on patterns of spatial and temporal variability of surface O<sub>3</sub> that ECHAM5-HAMMOZ seems able to capture (see also Pozzoli et al., 2011).

### 3.2 NAO and surface O<sub>3</sub>

#### 3.2.1 Measured surface O<sub>3</sub> and NAO correlation

During winter (December to February, DJF), the NAO impact on surface O<sub>3</sub> concentrations is remarkable: up to 8 out of 16 stations show a significant positive correlation between NAOI/PC1 and O<sub>3</sub> (Fig. 4). The significant positive correlations embrace the stations from Ireland to southern Norway and Sweden, to Central Europe. On the

## Model analysis and measurements intercomparison

F. S. R. Pausata et al.

Title Page

Abstract

Introduction

Conclusions

References

Tables

Figures

◀

▶

◀

▶

Back

Close

Full Screen / Esc

Printer-friendly Version

Interactive Discussion



other hand, in fall (September to November, SON) NAO and O<sub>3</sub> concentrations show the weakest correlation where only 3 stations have significant positive correlations.

In spring (March to May, MAM), O<sub>3</sub> concentrations in Ireland keep showing significant positive correlations with the NAO whereas in most of the stations in northern and central Europe the correlation weakens and become negative (mostly not significant). However the negative correlation in these areas are never significant. Weak negative correlations also appear in Portugal.

The summer season (June to August, JJA) displays the greatest difference between the NAOI/O<sub>3</sub> and the PC1/O<sub>3</sub> correlations. The NAOI/O<sub>3</sub> correlation turns out to be significant only in two stations located in southern Sweden (positive) and North Ireland (negative), whereas non-significant correlations are displayed in Central Europe (negative) and in the Iberian peninsula (positive). The PC1/O<sub>3</sub> correlation exhibits instead an opposite sign in central Europe and Ireland, and presents more locations with significant correlations compared to the NAOI/O<sub>3</sub> correlation. Significant positive PC1/O<sub>3</sub> correlations are found over the Iberian peninsula, Ireland, northern Germany and southern Scandinavia, whereas no negative correlations are found (Fig. 4).

### 3.2.2 Modeled surface O<sub>3</sub> and NAO correlation

In order to further investigate the correlation existing between NAO and surface O<sub>3</sub>, we turn to the model simulation that allows to better understand the correlation pattern over the whole Atlantic sector. To quantify the effects of the NAO onto surface O<sub>3</sub> concentrations, we also analyze surface ozone anomalies associated with an ensemble averages of high and low NAO phase winter and summer months. The ensemble averages are calculated considering O<sub>3</sub> concentration anomalies for each winter and summer month with normalized PC1 anomalies greater than 1 in absolute value (Table 2). While we have considered NAO and surface O<sub>3</sub> for all seasons, we have analyzed surface O<sub>3</sub> anomalies only in winter and summer, since they are the two extreme seasons: in winter the atmospheric dynamics plays the most important role in determining the O<sub>3</sub> variability, and in summer both dynamical and photochemical processes come into play, leading to dangerous O<sub>3</sub> concentrations.

## Model analysis and measurements intercomparison

F. S. R. Pausata et al.

Title Page

Abstract

Introduction

Conclusions

References

Tables

Figures



Back

Close

Full Screen / Esc

Printer-friendly Version

Interactive Discussion



Like the measurements, the model simulation shows the strongest and significant correlations between  $O_3$  concentrations and NAO in winter and the weakest correlations in fall over Europe (Fig. 5).

## Winter

5 The strong winter (DJF) influence of the NAO on surface  $O_3$  concentrations is mainly driven by large-scale atmospheric circulation and is not affected by the weak solar radiation and  $O_3$  photochemical reactions. As expected, the NAOI and the PC1 timeseries show a similar, however not identical, correlation pattern with simulated surface  $O_3$  concentrations. The significant positive correlations displayed over British Isles, Central Europe and southern Scandinavia match the correlation pattern obtained using the ground-station  $O_3$  measurements (cf. Figs. 4 and 5). The positive surface  $O_3$  anomalies up to 10 ppbv displayed in these areas (Fig. 6) during positive NAO phases are most likely due to transport of  $O_3$  enriched air masses from the Atlantic Ocean (Figs. 2 and 3). This long range low-level transport of enriched  $O_3$  air masses has also been shown by Li et al. (2002) for Mace Head using a model simulation with tracers. In contrast, the transport of  $O_3$  from the Atlantic Ocean is reduced over the Iberian Peninsula due to the expansion of the Azores anticyclone. The expansion of the Azores high carries down  $O_3$  depleted air masses from the European continent to the Italian peninsula and  $O_3$  enriched air from the Mediterranean Sea to Africa. This flow along the eastern flank of the anticyclone leads to lower-than-normal surface  $O_3$  concentrations over most of Italy (as can also be inferred by the measurements) and higher-than-normal surface  $O_3$  concentrations over north-eastern Africa (Figs. 5 and 6). The strengthening of the trade winds induced by a more vigorous Azores anticyclone, enhances the transport of depleted  $O_3$  air masses from the Sahara desert towards the coast of western Africa.

25 On the other hand, negative NAO phases are often associated with blocking events in the North Atlantic that reduce the contribution of  $O_3$  enriched air from the ocean and the  $O_3$  depleted flow from the European continent is more likely to make its way to the British Isles and western Europe. The negative phase of NAO leads to a southward

## Model analysis and measurements intercomparison

F. S. R. Pausata et al.

Title Page

Abstract

Introduction

Conclusions

References

Tables

Figures

◀

▶

◀

▶

Back

Close

Full Screen / Esc

Printer-friendly Version

Interactive Discussion



shift towards the Mediterranean Sea of the storm track and consequently, the O<sub>3</sub> enriched air masses from the Atlantic Ocean, increasing of few ppbv the surface O<sub>3</sub> concentrations in the western part of the Iberian peninsula (Fig. 6). More storms in the Mediterranean Sea enhance southerly flow towards Italy and northern Africa leading to a slightly increased surface O<sub>3</sub> concentrations over the Italian peninsula and decreased surface O<sub>3</sub> values in north-eastern Africa. The weakening of the trade winds associated with the low NAO phase may be not intense enough to lead to positive surface O<sub>3</sub> anomalies over western Africa: the SLP anomalies for the negative NAO phase over the Sahara desert and western Africa are in absolute values weaker than the SLP anomalies associated with the positive NAO phase (Fig. 6).

In the other seasons the NAOI/O<sub>3</sub> and the PC1/O<sub>3</sub> correlation patterns are different especially in summer as was also shown previously by the measurements (cf. JJA correlation patterns in Figs. 4 and 5). Moreover, the areas with significant NAOI/O<sub>3</sub> correlation are remarkably smaller than the areas with significant PC1/O<sub>3</sub> correlation. This strengthens the concept that the NAOI timeseries are not accurately capturing the seasonal shift of the atmospheric circulation.

## Spring

In spring (MAM), the PC1/O<sub>3</sub> correlation pattern is similar but somewhat weaker than in winter, with positive values over British Isles and Scandinavia in the north and north Africa in the south. The NAOI/O<sub>3</sub> also shows significant correlation over British Isles and part of Scandinavia, but the overall pattern starts becoming different compared to the PC1/O<sub>3</sub> correlation pattern. The weakening of the relationship between NAO and O<sub>3</sub> concentrations is in agreement with the data that show a reduced number of ground stations significantly correlated with the NAO (Fig. 4). However, the measurements show mostly negative correlations between NAO and O<sub>3</sub> concentrations over central-eastern Europe, whereas the model exhibits a weak positive correlation. It is worth to note that the PC1/O<sub>3</sub> correlations show less ground stations with negative values than the NAOI/O<sub>3</sub> correlations (Fig. 4). This is somehow consistent with the modeled

## Model analysis and measurements intercomparison

F. S. R. Pausata et al.

Title Page

Abstract

Introduction

Conclusions

References

Tables

Figures



Back

Close

Full Screen / Esc

Printer-friendly Version

Interactive Discussion



PC1/O<sub>3</sub> correlation patterns that exhibits broader areas positively correlated than the NAOI/O<sub>3</sub> pattern over central Europe (Fig. 5). Furthermore, given the fact that the correlations are mostly non-significant both for the model and the observed data the different correlation sign could be associated with the different period used to calculate the correlations in the model.

## Summer

During summer (JJA) the highest values of surface O<sub>3</sub> are simulated over central and southern Europe (Fig. 2) due to the interaction of atmospheric dynamics and photochemistry. The PC1/O<sub>3</sub> and NAOI/O<sub>3</sub> correlation patterns are remarkably different. The NAOI/O<sub>3</sub> correlations are only significantly positive over the Baltic region and in the southern tip of Spain. Negative correlations are shown over United Kingdom in agreement with the measurements. The PC1/O<sub>3</sub> correlation pattern shows instead a broad area of significant positive correlation that extends from western Africa up to the southern part of the British Isles. Significant negative correlations are displayed over the Adriatic sea. This different correlation behavior can also be inferred by the measurements in agreement with the simulated correlation patterns (cf. Figs. 4 and 5).

The significantly positive PC1/O<sub>3</sub> correlations are due to the expansion of the Azores high during positive phase of the NAO, embracing the Iberian Peninsula up to the British Isles (Figs. 1 and 6). The extension of the Azores anticyclone carries along its eastern flank continental air masses from western and central Europe, which are rich in O<sub>3</sub> precursors (Louka et al., 2003; Huntrieser and Schlager, 2004; Kulkarni et al., 2011), to Iberian Peninsula and Maghreb. The surface O<sub>3</sub> production in these areas is therefore enhanced also due to the ideal conditions of the Azores anticyclone associated with clear sky and high values of solar insolation. These more stable weather conditions account for the positive surface O<sub>3</sub> anomalies up to 8 ppbv over France, British Isles, North Sea and Baltic region (Fig. 6). The negative anomalies over Adriatic Sea (Figs. 5 and 6) simulated by the model during positive NAO phases, are associated with more unstable weather with enhanced precipitation (not shown) and reduced solar insolation over this area, and consequently reduced photochemical O<sub>3</sub> production.

## Model analysis and measurements intercomparison

F. S. R. Pausata et al.

Title Page

Abstract

Introduction

Conclusions

References

Tables

Figures

◀

▶

◀

▶

Back

Close

Full Screen / Esc

Printer-friendly Version

Interactive Discussion



The negative NAO phase leads to surface O<sub>3</sub> negative anomalies that are shifted south compared to positive anomalies, affecting western Africa, part of the Sahara desert and great part of the Mediterranean Sea, whereas mainly no anomalies are displayed in the Nordic Sea and Baltic Region (Fig. 6). The decreased O<sub>3</sub> concentrations over south-western Europe are caused by less O<sub>3</sub> enriched European continental flow induced by the negative NAO phase. The prevailing westerly air-mass flow associated with the negative NAO brings depleted O<sub>3</sub> air (Fig. 2) from the African continent towards the western and central Mediterranean Sea, causing over 10 ppbv negative O<sub>3</sub> anomalies.

## Fall

In fall (SON), both the PC1/O<sub>3</sub> and NAOI/O<sub>3</sub> correlations are mostly non-significant over Europe, except in the southern tip of Scandinavia and over part of the British Isles, in fair agreement with the measurements. In fall, the NAO accounts for less portion of the total variance of the atmospheric variability (Fig. 1) relative to the other seasons and therefore the link between atmospheric dynamics and O<sub>3</sub> concentrations is at the weakest.

### 3.3 NAO and O<sub>3</sub> aloft

Besides the long range transport of tropospheric air, the NAO may also influence transport of enriched air masses from the stratosphere into the troposphere, which may contribute to surface O<sub>3</sub> anomalies especially in winter and early spring.

Therefore, in this section we analyze O<sub>3</sub> anomalies through the depth of the troposphere associated with the ensemble averages of high and low NAO phase winter and summer months shown in Table 2.

In winter, during extreme NAO phases strong O<sub>3</sub> anomalies are displayed in the high-troposphere/lower-stratosphere that extend all the way down to the surface in central and northern Europe, and British Isles (Fig. 7). However, some of the mid-to-low

## Model analysis and measurements intercomparison

F. S. R. Pausata et al.

Title Page

Abstract

Introduction

Conclusions

References

Tables

Figures

◀

▶

◀

▶

Back

Close

Full Screen / Esc

Printer-friendly Version

Interactive Discussion



latitude O<sub>3</sub> anomalies seems instead more confined to the boundary layer, such as the anomalies over the Iberian Peninsula and Maghreb (Fig. 7 middle and bottom panels).

In summer, the stratospheric anomalies appears to be less pronounced and restricted to the high latitudes; nevertheless, some anomalies still extends from the high latitude lower stratosphere to the mid latitude troposphere (Fig. 8).

Deep STTs reaching the surface are rare (Stohl et al., 2003), however, Figs. 7 and 8 shows that in some areas O<sub>3</sub> anomalies extend all the way from the lower stratosphere/upper troposphere to the lower troposphere and may well be linked to changes in the number of STT events associated with the NAO phases. Unfortunately, since in our study we do not include a diagnostic for transport of stratospheric air into the troposphere, we could not quantify neither the amount of surface O<sub>3</sub> variability associated with the STT, nor the frequency of STT events associated with the NAO phases.

The anomalies that extend from the stratosphere to the surface may be due to two separate processes: (i) low level O<sub>3</sub> transport and/or photochemistry affect O<sub>3</sub> variability up to the mid troposphere; and (ii) STT affects O<sub>3</sub> variability down to the mid-to-high troposphere. The anomalies in the mid-to-high troposphere can eventually reach the surface on longer time scale influencing the overall climatology and budget. This is consistent with Hocking et al. (2007) that have shown the importance of STT events for overall surface baseline ozone budget rather than for short term surface O<sub>3</sub> variability. Hence, whether a given NAO phase persists for several years in a row to the detriment of the other phase, STTs may be responsible for long term trends in surface O<sub>3</sub> concentrations.

## 4 Discussion

We have described the relationship existing between atmospheric dynamics and O<sub>3</sub> concentrations throughout the year using both measurements from ground stations spread over Europe and a coupled atmosphere-chemistry model.

### Model analysis and measurements intercomparison

F. S. R. Pausata et al.

Title Page

Abstract

Introduction

Conclusions

References

Tables

Figures

◀

▶

◀

▶

Back

Close

Full Screen / Esc

Printer-friendly Version

Interactive Discussion



**Model analysis and  
measurements  
intercomparison**

F. S. R. Pausata et al.

Title Page

Abstract

Introduction

Conclusions

References

Tables

Figures

◀

▶

◀

▶

Back

Close

Full Screen / Esc

Printer-friendly Version

Interactive Discussion



Our study shows that the NAO is able to affect  $O_3$  concentrations in many areas of Europe in all seasons, except in fall. However, while the standard method of characterizing the NAO, i.e. the station-based NAO index, captures the atmosphere circulation/ $O_3$  concentrations relationship in winter and spring, it fails in summer. On the other hand, we show that the Empirical Orthogonal Function-based index (PC1) is able to detect the NAO/ $O_3$  relationship not only in winter and spring but also in summer. This behavior is due to the fact the EOF analysis takes into account the seasonal shifting of the NAO centers of action throughout the year, in contrast to the station-based NAOI which is fixed in space. Our study shows that the NAOI is a useful metric when addressing correlations with winter/early spring atmospheric circulation, because it provides similar or even better results (Figs. 4 and 5) and it is an easier analysis tool compared to the EOF analysis. For the summer months, instead, the PC1/ $O_3$  correlations show superior results and the PC1 timeseries should be used rather than the NAOI (see for example Fig. 5): the two stations used to calculate the NAOI are not representative of the summer atmospheric circulation anymore since the NAO centers of action in this season are shifted northwards compared to winter (Fig. 1). Therefore, an interpretation of the NAOI/ $O_3$  correlation pattern in other seasons than winter may be difficult and lead to erroneous conclusions that in some areas or seasons there is no relationship between the NAO and surface  $O_3$  concentrations.

Correlations between NAO and surface  $O_3$  concentrations are interesting from a general standpoint, but they could also be used as a tool for inferring areas more exposed to extreme  $O_3$  pollution events during summer. The NAO has a lingering forecast skill at intraseasonal (3 to 6 weeks) time scale (Johansson, 2007). The information about forthcoming NAO behaviors can be translated to which PC1 values can be expected and therefore, it can be used to identify areas at risk of high  $O_3$  concentrations, without performing costly chemical weather forecasting at monthly timescale.

On interannual to decadal timescales the PC1 timeseries tendency may be used to understand observed  $O_3$  background trends and variability: if a specific NAO phase persists for several years the induced  $O_3$  anomalies (Fig. 6) may effect the background

climatological surface O<sub>3</sub>.

Surface O<sub>3</sub> measurements have shown an upward trend in central and northern Europe (Monk, 2003; Simmonds et al., 2004; Jonson et al., 2006; Cui et al., 2011; Wilson et al., 2012) especially in winter months in the 1990s in good agreements with modeled O<sub>3</sub> concentrations (see Fig. 9 and Pozzoli et al., 2011). Pozzoli et al. (2011) have also shown an increase in modeled surface O<sub>3</sub> concentrations over Europe during the period 1980–2005 even when the anthropogenic emissions of O<sub>3</sub> precursors were kept at constant levels. They attributed the surface O<sub>3</sub> concentration increase to changes in natural emissions and meteorology without providing further analysis of the underlying drivers. As seen in Sect. 3.1, the NAO had a persisting positive phase from the late 1980s until the end of the 1990s in three out of four seasons and we show that the NAO positive phase leads to positive surface O<sub>3</sub> anomalies up to 8 ppbv on average in great part of western and northern Europe. Wilson et al. (2012) have demonstrated how individual years have a significant impact on ozone trends when calculated over short timescale (10–15 yr). Therefore, the NAO behavior and the associated surface O<sub>3</sub> anomalies may explain the trend reported at Mace Head (Fig. 9) and over western and northern Europe. Moreover, the O<sub>3</sub> trend at Mace Head is more pronounced in winter and spring seasons when the STT is also at the maximum (Holton et al., 1995): Figs. 7 and 8 show how positive NAO phases lead to O<sub>3</sub> anomalies that extend from the lower stratosphere/upper troposphere to the surface; this could indicate increased STT over northern Europe during the positive NAO phases – as also shown by Sprenger and Wernli (2003) – that eventually may affect the overall surface O<sub>3</sub> budget. Finally, the trend in surface O<sub>3</sub> at Mace Head has flattened since 2000 (Fig. 9) following the NAO tendency towards less positive NAO phases (<http://www.cgd.ucar.edu/cas/jhurrell/indices.info.html#naostatann>). This further corroborates the potential influence of the NAO on surface O<sub>3</sub> budgets in western and northern Europe.

An important implication is that under climate change conditions, with increasing greenhouse gas concentrations in the next decades, several model simulations (e.g.

**Model analysis and measurements intercomparison**

F. S. R. Pausata et al.

Title Page

Abstract

Introduction

Conclusions

References

Tables

Figures



Back

Close

Full Screen / Esc

Printer-friendly Version

Interactive Discussion



Kuzmina et al., 2005; Stephenson and Pavan, 2006) predict a positive wintertime NAO trend. Recently Bladé et al. (2012) have shown that also the summer NAO may prefer the positive state in the future, extending the observed positive trend started in 1967 (see Fig. 1 in Hurrell and Folland, 2002). While the wintertime NAO trends may be fundamental for the overall O<sub>3</sub> concentrations, the summertime NAO trends are extremely important for central-western and southwestern Europe, with potential influence in eastern US and Canada as well (Figs. 5 and 6). The positive summer NAO trend between the 70s and 90s has caused a change toward persistent anticyclonic flow (Hurrell and Folland, 2002) and it corresponded to an increase in mean central England temperatures. Greatbach and Rong (2006) found that a strong correlation between summer NAO and central England temperature holds for much of the twentieth century. The increased summer NAOI also led to a lowering of precipitation over much of Northern Europe. As seen in Sect. 3.1, this meteorological pattern favors positive surface O<sub>3</sub> anomalies from the Iberian peninsula up to the British Isles and Baltic region (Fig. 6). If the positive trend in summer NAO persists, these areas will likely be more frequently exposed to higher-than-normal O<sub>3</sub> concentrations with consequences for O<sub>3</sub> abatement strategies.

Our study highlights the importance of the NAO in driving surface ozone variability in large parts of Europe, not only affecting low level transport but also middle and upper troposphere and stratosphere-to-troposphere transport. However, a quantitative analysis on the relative impact of STTs and low level transport associated to the NAO phases on surface ozone concentrations was not possible using our chemical re-analysis model simulation, due to a lack of appropriate diagnostic tools. We therefore strongly recommend that future studies using climate-chemistry models are supplemented with appropriate diagnostics (e.g. tracers) to investigate more in depth the effects of each NAO phase on surface ozone interannual and decadal variability and trend, especially – but not only – in summer when ozone concentrations peak and only few studies are available. To correctly characterize the NAO in all seasons, the EOF analysis of the SLP field and the associated PC1 should be adopted.

## Model analysis and measurements intercomparison

F. S. R. Pausata et al.

[Title Page](#)[Abstract](#)[Introduction](#)[Conclusions](#)[References](#)[Tables](#)[Figures](#)[⏪](#)[⏩](#)[◀](#)[▶](#)[Back](#)[Close](#)[Full Screen / Esc](#)[Printer-friendly Version](#)[Interactive Discussion](#)

## 5 Conclusions

In this study, we analyze how the atmospheric general circulation influences ozone concentrations in Europe at the surface and through the depth of the troposphere and lower stratosphere, using ground station measurements and a coupled atmosphere-chemistry model for the period 1980–2005. The main findings are:

- The North Atlantic Oscillation (NAO) influences surface ozone concentrations over Europe in all seasons except in fall, when significant positive correlation between the NAO and surface ozone are detected only in part of the British Isles and southern Scandinavia.
- The standard NAO Index (NAOI) is a good atmospheric circulation predictor for surface ozone concentrations in winter over Europe, whereas it fails in summer; therefore, it is a simple and attractive metric to analyze variability of atmospheric trace gases connected with winter and early spring atmospheric circulation.
- The PC1 timeseries associated with the Empirical Orthogonal Function analysis of the sea level pressure field, is the best atmospheric circulation predictor for surface ozone concentrations in summer over Europe and it could also be used to detect sensitive areas to forthcoming ozone pollution spells.
- The NAO behavior in the last decades could have been responsible for or at least had an influence on the positive trend in surface ozone concentration seen over northern and western Europe.

*Acknowledgements.* This work was funded by the European Community's Seventh Framework Program (FP7) in the project PEGASOS. The simulations were performed on the computers at Deutsches Klimarechenzentrum (DKRZ). We would like to thank the EMEP network for providing ozone measurements over Europe, in particularly Gerard Spain and Simon O'Doherty.

### Model analysis and measurements intercomparison

F. S. R. Pausata et al.

Title Page

Abstract

Introduction

Conclusions

References

Tables

Figures

◀

▶

◀

▶

Back

Close

Full Screen / Esc

Printer-friendly Version

Interactive Discussion



## References

- Akimoto, H: Global air quality and pollution, *Science*, 302, 1716–1719, 2003 3132
- Auvray, M., Bey, I., Lull, E., Schultz, M. G., and Rast, S.: A model investigation of tropospheric ozone chemical tendencies in long-range transported pollution plumes, *J. Geophys. Res.*, 112, D05304, doi:10.1029/2006JD007137, 2007. 3137
- Barnston, A. G. and Livezey, R. E.: Classification, seasonality and persistence of low-frequency atmospheric circulation patterns, *Mon. Weather Rev.*, 115, 1083–1126, 1987. 3134
- Bladé, I., Liebmann, B., Fortuny, D., and van Oldenborgh, G. J.: Observed and simulated impacts of the summer NAO in Europe: Implications for projected drying in the Mediterranean region, *Clim. Dyn.*, doi:10.1007/s00382-011-1195-x, in press, 2012. 3149
- Bronnimann, S., Luterbacher, J., Schmutz, C., Wanner, H., and Staehelin, J.: Variability of total ozone at Arosa, Switzerland, since 1931 related to atmospheric circulation indices, *Geophys. Res. Lett.*, 27, 2213–2216, 2000. 3133
- Bronnimann, S., Buchmann, B., and Wanner, H.: Trends in near-surface ozone concentrations in Switzerland: the 1990s, *Atmos. Environ.*, 36, 2841–2852, 2002. 3133
- Creilson, J. K., Fishman, J., and Wozniak, A. E.: Intercontinental transport of tropospheric ozone: a study of its seasonal variability across the North Atlantic utilizing tropospheric ozone residuals and its relationship to the North Atlantic Oscillation, *Atmos. Chem. Phys.*, 3, 2053–2066, doi:10.5194/acp-3-2053-2003, 2003. 3133, 3135
- Christoudias, T., Pozzer, A., and Lelieveld, J.: Influence of the North Atlantic Oscillation on air pollution transport, *Atmos. Chem. Phys.*, 12, 869–877, doi:10.5194/acp-12-869-2012, 2012. 3135
- Cui, J., Pandey Deolal, S., Sprenger, M., Henne, S., Staehelin, J., Steinbacher, M., and Nédélec, P.: Free tropospheric ozone changes over Europe as observed at Jungfraujoch (1990–2008): An analysis based on backward trajectories, *J. Geophys. Res.*, 116, D10304, doi:10.1029/2010JD015154, 2011. 3148
- Dentener, F., Stevenson, D., Ellingsen, K., van Noije, T., Schultz, M., Amann, M., Atherton, C., Bell, N., Bergmann, D., Bey, I., Bouwman, L., Butler, T., Cofala, J., Collins, B., Drevet, J., Doherty, R., Eickhout, B., Eskes, H., Fiore, A., Gauss, M., Hauglustaine, D., Horowitz, L., Isaksen, I. S. A., Josse, B., Lawrence, M., Krol, M., Lamarque, J. F., Montanaro, V., Müller, J. F., Peuch, V. H., Pitari, G., Pyle, J., Rast, S., Rodriguez, J., Sanderson, M., Savage, N. H., Shindell, D., Strahan, S., Szopa, S., Sudo, K., Van Dingenen, R., Wild, O. and Zeng,

ACPD

12, 3131–3167, 2012

### Model analysis and measurements intercomparison

F. S. R. Pausata et al.

Title Page

Abstract

Introduction

Conclusions

References

Tables

Figures

◀

▶

◀

▶

Back

Close

Full Screen / Esc

Printer-friendly Version

Interactive Discussion



**Model analysis and  
measurements  
intercomparison**

F. S. R. Pausata et al.

Title Page

Abstract

Introduction

Conclusions

References

Tables

Figures

◀

▶

◀

▶

Back

Close

Full Screen / Esc

Printer-friendly Version

Interactive Discussion



G.: The global atmospheric environment for the next generation, *Environ. Sci. Technol.*, 40, 3586–3594, 2006 3132

Duncan B. N. and Bey, I.: A modeling study of the export pathways of pollution from Europe: Seasonal and interannual variations (1987–1997), *J. Geophys. Res.-Atmos.*, 109, D08301, doi:10.1029/2003JD004079, 2004. 3135, 3136

Eckhardt, S., Stohl, A., Beirle, S., Spichtinger, N., James, P., Forster, C., Junker, C., Wagner, T., Platt, U., and Jennings, S. G.: The North Atlantic Oscillation controls air pollution transport to the Arctic, *Atmos. Chem. Phys.*, 3, 1769–1778, doi:10.5194/acp-3-1769-2003, 2003. 3135

Ellingsen, K., Gauss, M., Van Dingenen, R., Dentener, F. J., Emberson, L., Fiore, A. M., Schultz, M. G., Stevenson, D. S., Ashmore, M. R., Atherton, C. S., Bergmann, D. J., Bey, I., Butler, T., Drevet, J., Eskes, H., Hauglustaine, D. A., Isaksen, I. S. A., Horowitz, L. W., Krol, M., Lamarque, J. F., Lawrence, M. G., van Noije, T., Pyle, J., Rast, S., Rodriguez, J., Savage, N., Strahan, S., Sudo, K., Szopa, S., and Wild, O.: Global ozone and air quality: a multi-model assessment of risks to human health and crops, *Atmos. Chem. Phys. Discuss.*, 8, 2163–2223, doi:10.5194/acpd-8-2163-2008, 2008. 3137

Fehsenfeld, F. C., Daum, P., Leatch, W. R., Trainer, M., Parrish, D. D., and Hubler, G.: Transport and processing of O<sub>3</sub> and O<sub>3</sub> precursors over the North Atlantic: An overview of the 1993 North Atlantic Regional Experiment (NARE) summer intensive, *J. Geophys. Res.-Atmos.*, 101, 28877–28891, 1996. 3133

Fishman, J., Wozniak, A. E., and Creilson, J. K.: Global distribution of tropospheric ozone from satellite measurements using the empirically corrected tropospheric ozone residual technique: Identification of the regional aspects of air pollution, *Atmos. Chem. Phys.*, 3, 893–907, doi:10.5194/acp-3-893-2003, 2003. 3140

Fyfe, J. C., Boer, G. J., and Flato, G. M.: The Arctic and Antarctic oscillations and their projected changes under global warming, *Geophys. Res. Lett.*, 26, 1601–1604, 1999. 3135

Gillett, N. P., Baldwin, M. P., and Allen, M. R.: Evidence for nonlinearity in observed stratospheric circulation changes, *J. Geophys. Res.-Atmos.*, 106, 7891–7901, 2001. 3135

Greatbatch, R. J. and Rong, P. P.: Discrepancies between different Northern Hemisphere summer atmospheric circulation data products, *J. Clim.*, 19, 1261–1273, 2006. 3149

Hagemann, S., Arpe, K., and Roeckner, E.: Evaluation of the Hydrological Cycle in the ECHAM5 Model, *J. Climate*, 19, 3810–3827, 2006. 3137

Hess, P. G. and Lamarque, J.-F.: Ozone source attribution and its modulation by the Arctic oscillation during the spring months, *J. Geophys. Res.-Atmos.*, 112, D11303,

doi:10.1029/2006JD007557, 2007. 3135

Hess, P. and Mahowald, N.: Interannual variability in hindcasts of atmospheric chemistry: the role of meteorology, *Atmos. Chem. Phys.*, 9, 5261–5280, doi:10.5194/acp-9-5261-2009, 2009. 3138

5 Hocking, W. K., Carey-Smith, T., Tarasick, D., Argall, S., Strong, K., Rochon, Y., Zawadzki, I., and Taylor, P. A.: Detection of Stratospheric Ozone Intrusions by Windprofiler Radars, *Nature*, 450, 281–284, 2007. 3133, 3146

Holton, J. R., Haynes, P. H., McIntyre, M. E., Douglass, A. R., Rood, R. B., and Pfister, L.: Stratosphere-troposphere exchange, *Rev. Geophys.*, 33, 403–439, 1995. 3148

10 Horowitz, L., Walters, S., Mauzerall, D., Emmons, L., Rasch, P., Granier, C., Tie, X., Lamarque, J., Schultz, M., Tyndall, G., Orlando, J., and Brasseur, G.: A global simulation of tropospheric ozone and related tracers: Description and evaluation of MOZART, version 2, *J. Geophys. Res.-Atmos.*, 108, 4784, doi:10.1029/2002JD002853, 2003. 3137

Hurrell, J. W.: Decadal trends in the North Atlantic Oscillation: regional temperatures and precipitation, *Science*, 269, 676–679, 1995. 3134

Hurrell, J. W. and Folland, C. K.: A Change in the Summer Atmospheric Circulation over the North Atlantic, *CLIVAR Exchanges*, 25, 52–54, 2002.

Hurrell, J. W., Kushnir, Y., Ottersen, G., and Visbeck, M.: The North Atlantic Oscillation: climatic significance and environmental impact, *An overview of the North Atlantic Oscillation*, AGU monograph, 13, 1–35, 2003.

20 Jeuken, A., Siegmund, P., Heijboer, L., Feichter, J., and Bengtsson, L.: On the potential of assimilating meteorological analyses in a global climate model for the purpose of model validation, *J. Geophys. Res.*, 101, 16939–16950, 1996. 3137

Johansson, Å.: Prediction skill of the NAO and PNA from daily to seasonal time scales, *J. Clim.*, 20, 1957–1975, 2007. 3147

25 Jonson, J. E., Simpson, D., Fagerli, H., and Solberg, S.: Can we explain the trends in European ozone levels?, *Atmos. Chem. Phys.*, 6, 51–66, doi:10.5194/acp-6-51-2006, 2006. 3148

Kuzmina, S. I., Bengtsson, L., Johannessen, O. M., Drange, H., Bobylev, L. P., and Miles, M. W.: The North Atlantic Oscillation and greenhouse-gas forcing, *Geophys. Res. Lett.*, 32, L04703, doi:10.1029/2004GL021064, 2005. 3136, 3149

30 Lelieveld, J. and Dentener, F. J.: What controls tropospheric ozone?, *J. Geophys. Res.*, 105, 3531–3551, 2000. 3133

Li, Q. B., Jacob, D. J., Bey, I., Palmer, P. I., Duncan, B. N., Field, B. D., Martin, R. V., Fiore, A. M.,

**Model analysis and measurements intercomparison**

F. S. R. Pausata et al.

Title Page

Abstract

Introduction

Conclusions

References

Tables

Figures

◀

▶

◀

▶

Back

Close

Full Screen / Esc

Printer-friendly Version

Interactive Discussion



## Model analysis and measurements intercomparison

F. S. R. Pausata et al.

Title Page

Abstract

Introduction

Conclusions

References

Tables

Figures

◀

▶

◀

▶

Back

Close

Full Screen / Esc

Printer-friendly Version

Interactive Discussion



Yantosca, R. M., Parrish, D. D., Simmonds, P. G., Oltmans, S. J.: Transatlantic transport of pollution and its effects on surface ozone in Europe and North America, *J. Geophys. Res.*, 107, 4166, doi:10.1029/2001JD001422, 2002. 3133, 3135, 3136

Lövblad, G., Tarrasón, L., Torseth, K., and Dutchak, S.: EMEP Assessment, part 1: European perspective, *Norw. Meteorol. Inst., Oslo*, 2004. 3132

Monk, P. S.: TROTREP Synthesis and Integration Report. Report to the EU FPV Energy, Environment and Sustainable Development Program., European Union, 2003. 3148

Parrish, D. D., Ryerson, T. B., Holloway, J. S., Frost, G. J., and Fehsenfeld, F. C.: Export of North American ozone pollution to the North Atlantic Ocean, *Science*, 259, 1436–1439, 1993. 3133

Pozzoli, L., Bey, I., Rast, S., Schultz, M. G., Stier, P., and Feichter, J.: Trace gas and aerosol interactions in the fully coupled model of aerosol-chemistry-climate ECHAM5-HAMMOZ: 1. Model description and insights from the spring 2001 TRACE-P experiment, *J. Geophys. Res.*, 113, D07308, doi:10.1029/2007JD009007, 2008a. 3137

Pozzoli, L., Bey, I., Rast, S., Schultz, M. G., Stier, P., and Feichter, J.: Trace gas and aerosol interactions in the fully coupled model of aerosol-chemistry-climate ECHAM5-HAMMOZ: 2. Impact of heterogeneous chemistry on the global aerosol distributions, *J. Geophys. Res.*, 113, D07309, doi:10.1029/2007JD009008, 2008b. 3137

Pozzoli, L., Janssens-Maenhout, G., Diehl, T., Bey, I., Schultz, M. G., Feichter, J., Vignati, E., and Dentener, F.: Re-analysis of tropospheric sulfate aerosol and ozone for the period 1980–2005 using the aerosol-chemistry-climate model ECHAM5-HAMMOZ, *Atmos. Chem. Phys.*, 11, 9563–9594, doi:10.5194/acp-11-9563-2011, 2011. 3137, 3140, 3148

Rast, J., Schultz, M., Aghedo, A., Bey, I., Brasseur, G., Diehl, T., Esch, M., Ganzeveld, L., Kirchner, I., Kornblueh, L., Rhodin, A., Roeckner, E., Schmidt, H., Schroede, S., Schulzweida, U., Stier, P., and van Noije, T.: Evaluation of the tropospheric chemistry general circulation model ECHAM5–MOZ and its application to the analysis of the inter-annual variability in tropospheric ozone from 1960–2000 chemical composition of the troposphere for the period 1960–2000 (RETRO), *MPI-Report (Reports on Earth System Science)*, in preparation, 2012. 3137

Roeckner, E., Bauml, G., Bonaventura, L., Brokopf, R., Esch, M., Giorgetta, M., Hagemann, S., Kirchner, I., Kornblueh, L., Manzini, E., Rhodin, A., Schlese, U., Schulzweida, U., and Tompkins, A.: The atmospheric general circulation model ECHAM5: Part 1, *Tech. Rep. 349*, Max Planck Institute for Meteorology, Hamburg, 2003. 3137

Roeckner, E., Brokopf, R., Esch, M., Giorgetta, M., Hagemann, S., Kornblueh, L., Manzini, E.,

## Model analysis and measurements intercomparison

F. S. R. Pausata et al.

Title Page

Abstract

Introduction

Conclusions

References

Tables

Figures

◀

▶

◀

▶

Back

Close

Full Screen / Esc

Printer-friendly Version

Interactive Discussion



- Schlese, U., and Schulzweida, U.: Sensitivity of Simulated Climate to Horizontal and Vertical Resolution in the ECHAM5 Atmosphere Model, *J. Climate*, 19, 3771–3791, 2006. 3137
- Simmonds, P. G., Derwent, R. G., Manning, A. L. and Spain, G.: Significant growth in surface ozone at Mace Head, Ireland, 1987–2003, *Atmos. Environ.*, 38, 4769–4778, 2004. 3133, 3148
- 5 Sprenger, M., and Wernli, H.: A northern hemispheric climatology of cross-tropopause exchange for the ERA15 time period (1979–1993), *J. Geophys. Res.*, 108, 8521, doi:10.1029/2002JD002636, 2003. 3135, 3148
- Stephenson, D. B. and Pavan, V., and Collins, M., and Junge, M. M., and Quadrelli, R.: North Atlantic Oscillation response to transient greenhouse gas forcing and the impact on European winter climate: a CMIP2 multi-model assessment, *Clim. Dyn.*, 27, 401–420, 2006. 3136, 3149
- 10 Stevenson, D., Dentener, F., Schultz, M., Ellingsen, K., van Noije, T., Wild, O., Zeng, G., Amann, M., Atherton, C., Bell, N., Bergmann, D., Bey, I., Butler, T., Cofala, J., Collins, W., Derwent, R., Doherty, R., Drevet, J., Eskes, H., Fiore, A., Gauss, M., Hauglustaine, D., Horowitz, L., Isaksen, I., Krol, M., Lamarque, J., Lawrence, M., Montanaro, V., Muller, J., Pitari, G., Prather, M., Pyle, J., Rast, S., Rodriguez, J., Sanderson, M., Savage, N., Shindell, D., Strahan, S., Sudo, K., and Szopa, S.: Multimodel ensemble simulations of present-day and near-future tropospheric ozone, *J. Geophys. Res.-Atmos.*, 111, D08301, doi:10.1029/2005JD006338, 2006. 3138
- 20 Stier, P., Feichter, J., Kinne, S., Kloster, S., Vignati, E., Wilson, J., Ganzeveld, L., Tegen, I., Werner, M., Balkanski, Y., Schulz, M., Boucher, O., Minikin, A., and Petzold, A.: The aerosol-climate model ECHAM5-HAM, *Atmos. Chem. Phys.*, 5, 1125–1156, doi:10.5194/acp-5-1125-2005, 2005. 3137
- 25 Stohl, A., Bonasoni, P., Cristofanelli, P., Collins, W., Feichter, J., Frank, A., Forster, C., Gerasopoulos, E., Gaggeler, H., James, P., Kentarchos, T., Kromp-Kolb, H., Kruger, B., Land, C., Meloan, J., Papayannis, A., Priller, A., Seibert, P., Sprenger, M., Roelofs, G. J., Scheel, H. E., Schnabel, C., Siegmund, P., Tobler, L., Trickl, T., Wernli, H., Wirth, V., Zanis, P., and Zerefos, C.: Stratosphere-troposphere exchange: A review, and what we have learned from STACCATO, *J. Geophys. Res.-Atmos.*, 108, 8516, doi:10.1029/2002JD002490, 2003. 3133, 3146
- 30 Uppala, S. M., Kållberg, P. W., Simmons, A. J., Andrae, U., Bechtold, V. D. C., Fiorino, M., Gibson, J. K., Haseler, J., Hernandez, A., Kelly, G. A., Li, X., Onogi, K., Saarinen, S., Sokka,

## Model analysis and measurements intercomparison

F. S. R. Pausata et al.

Title Page

Abstract

Introduction

Conclusions

References

Tables

Figures

◀

▶

◀

▶

Back

Close

Full Screen / Esc

Printer-friendly Version

Interactive Discussion



- N., Allan, R. P., Andersson, E., Arpe, K., Balmaseda, M. A., Beljaars, A. C. M., Berg, L. V. D., Bidlot, J., Bormann, N., Caires, S., Chevallier, F., Dethof, A., Dragosavac, M., Fisher, M., Fuentes, M., Hagemann, S., Hólm, E., Hoskins, B. J., Isaksen, L., Janssen, P. A. E. M., Jenne, R., McNally, A. P., Mahfouf, J.-F., Morcrette, J.-J., Rayner, N. A., Saunders, R. W., Simon, P., Sterl, A., Trenberth, K. E., Untch, A., Vasiljevic, D., Viterbo, P., and Woollen, J.: The ERA-40 re-analysis, *Q. J. Roy. Meteorol. Soc.*, 131, 2961–3012, 2005. 3137
- Walker, G.T.: Correlation in seasonal variation of weather, IX: A further study of world weather, *Mem. Indian Meteor. Dep.*, 24, 275–332, 1924. 3133
- Walker, G. T. and Bliss, E. W.: World Weather, V. *Mem. R. Meteorol. Soc.*, 4, 53–83, 1932. 3133
- Wallace, M.: North Atlantic Oscillation/annular mode: Two paradigms - one phenomenon, *Q. J. Roy. Meteor. Soc.*, 126, 791–805, 2000. 3135
- Wilson, R. C., Fleming, Z. L., Monks, P. S., Clain, G., Henne, S., Konovalov, I. B., Szopa, S., and Menut, L.: Have primary emission reduction measures reduced ozone across Europe? An analysis of European rural background ozone trends 1996–2005, *Atmos. Chem. Phys.*, 12, 437–454, doi:10.5194/acp-12-437-2012, 2012. 3148

## Model analysis and measurements intercomparison

F. S. R. Pausata et al.

Title Page

Abstract

Introduction

Conclusions

References

Tables

Figures

◀

▶

◀

▶

Back

Close

Full Screen / Esc

Printer-friendly Version

Interactive Discussion



**Table 1.** Ground stations with geographical coordinates and years used in the analysis.

Station	Latitude	Longitude	Altitude (a.s.l.)	Years
Viznar (Spain)	37° 14'00" N	03° 32'00" W	1265 m	1995–2005
Monte Velho (Portugal)	38° 05'00" N	08° 48'00" W	43 m	1990–2005
Montelibretti (Italy)	42° 06'00" N	12° 38'00" E	48 m	1995–2005
Illmitz (Austria)	47° 46'00" N	16° 46'00" E	117 m	1990–2005
Donon (France)	48° 30'00" N	07° 08'00" E	775 m	1995–2005
Eupen (Belgium)	50° 37'46" N	06° 00'10" E	295 m	1990–2005
Yarner Wood (England)	50° 35'47" N	03° 42'47" W	119 m	1990–2005
Mace Head (Ireland)	53° 10'00" N	09° 30'00" W	15 m	1990–2005
Lough Navar (North. Ireland)	54° 26'35" N	07° 12'52" W	126 m	1990–2005
Sniezka (Poland)	50° 44'00" N	15° 44'00" E	1603 m	1995–2005
Leba (Poland)	54° 45'00" N	17° 32'00" E	2 m	1995–2005
Langenbrugge (Germany)	52° 48'08" N	10° 45'34" E	74 m	1990–2005
Neuglobsow (Germany)	53° 10'00" N	13° 02'00" E	62 m	1991–2005
Westerland (Germany)	54° 55'32" N	08° 18'35" E	12 m	1990–2005
Rørwik (Sweden)	57° 25'00" N	11° 56'00" E	10 m	1990–2002
Råö (Sweden)	57° 23'38" N	11° 54' 50" E	5 m	2003–2005
Birkenes (Norway)	58° 23'00" N	08° 15'00" E	190 m	1990–2005

## Model analysis and measurements intercomparison

F. S. R. Pausata et al.

**Table 2.** Winter and summer months with the associated normalized PC1 used for calculating the ensemble average for positive and negative NAO phase.

Winter (DJF)			Summer (JJA)								
NAO–		NAO+	NAO–		NAO+						
month	year	index	month	year	index						
Jan	1980	–1.6	Dec	1982	+1.0	Jul	1980	–1.4	Jul	1982	+1.0
Dec	1981	–1.4	Jan	1983	+1.3	Jun	1982	–2.0	Jun	1983	+1.6
Jan	1982	–1.2	Dec	1988	+1.0	Aug	1985	–1.1	Aug	1983	+1.3
Jan	1985	–2.0	Jan	1989	+1.3	Aug	1986	–1.1	Jun	1986	+1.4
Feb	1985	–1.6	Feb	1989	+1.8	Jun	1987	–1.8	Jun	1988	+1.5
Dec	1985	–1.2	Feb	1990	+2.3	Aug	1987	–1.8	Jun	1989	+1.1
Feb	1986	–2.3	Dec	1991	+1.1	Jun	1993	–1.1	Jul	1989	+1.8
Jan	1987	–1.1	Jan	1993	+2.2	Jul	1993	–2.0	Aug	1991	+2.0
Feb	1987	–1.3	Feb	1995	+1.3	Jun	1997	–1.5	Jun	1994	+2.4
Dec	1995	–1.4	Feb	1997	+1.5	Jun	1998	–2.1	Jul	1994	+1.3
Jan	1996	–1.6	Feb	2000	+1.2	Aug	1999	–1.0	Aug	1994	+1.4
Jan	1998	–1.1	Dec	2004	+1.6	Aug	2004	–1.1	Jul	1996	+1.6
Dec	2000	–1.0							Jun	1999	+2.0
Dec	2001	–1.1									
Dec	2002	–1.1									

Title Page

Abstract

Introduction

Conclusions

References

Tables

Figures

⏪

⏩

◀

▶

Back

Close

Full Screen / Esc

Printer-friendly Version

Interactive Discussion



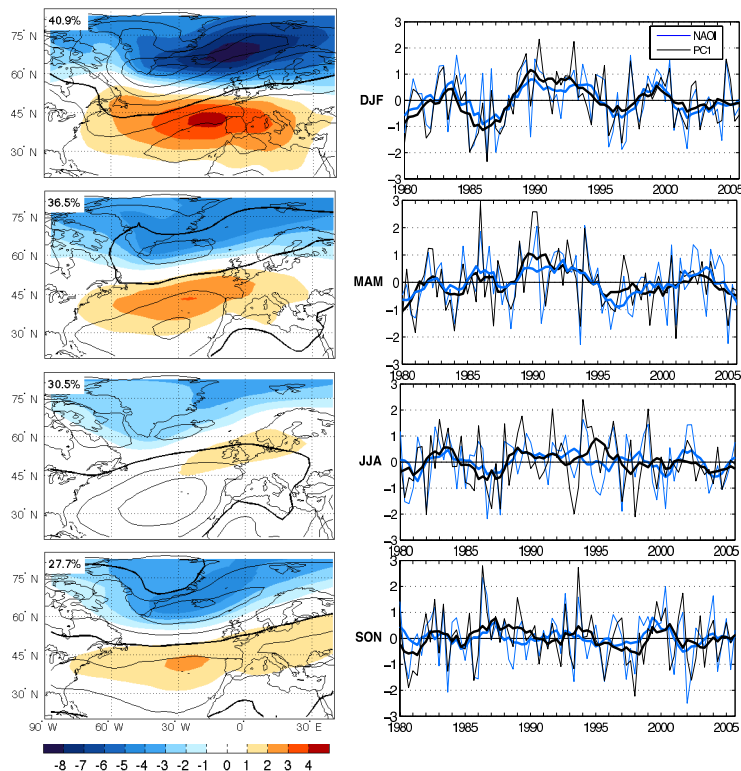


**Fig. 1.** Left panels: simulated leading EOF of monthly SLP anomalies (colored shading: hPa/standard deviation of PC) using data from all months of each season and SLP mean (contours: 4 hPa interval from 998 to 1022 hPa; bold contour denotes 1014 hPa) in the North Atlantic sector. The EOF patterns represent the SLP anomalies associated with normalized PC1 equal 1 for the NAO positive phase (opposite sign for the NAO negative phase). Bold numbers show the amount of variance explained by the first EOF as a percentage of the total variance. Right panels: NAOI (blue) and normalized PC1 (black) timeseries for each season. The bold lines show the 6-month (2 seasons) running mean.

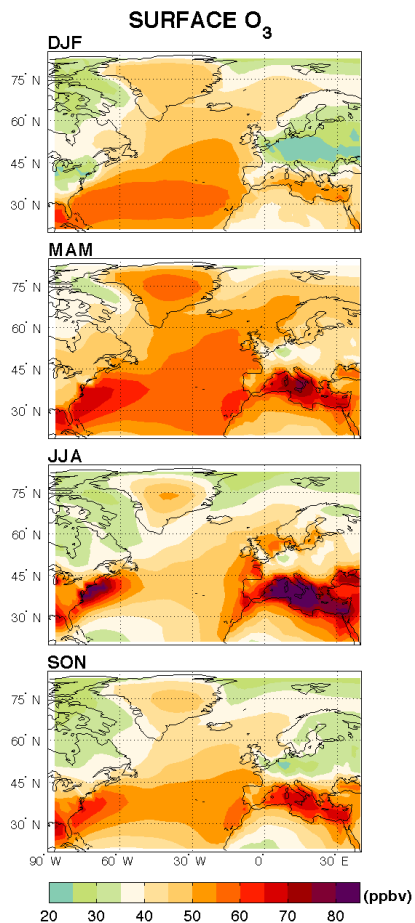


**Fig. 2.** Climatological (1980–2005) modeled surface O<sub>3</sub> concentrations for each season.

**Model analysis and measurements intercomparison**

F. S. R. Pausata et al.

Title Page

Abstract Introduction

Conclusions References

Tables Figures

◀ ▶

◀ ▶

Back Close

Full Screen / Esc

Printer-friendly Version

Interactive Discussion



**Model analysis and  
measurements  
intercomparison**

F. S. R. Pausata et al.

Title Page

Abstract

Introduction

Conclusions

References

Tables

Figures

◀

▶

◀

▶

Back

Close

Full Screen / Esc

Printer-friendly Version

Interactive Discussion

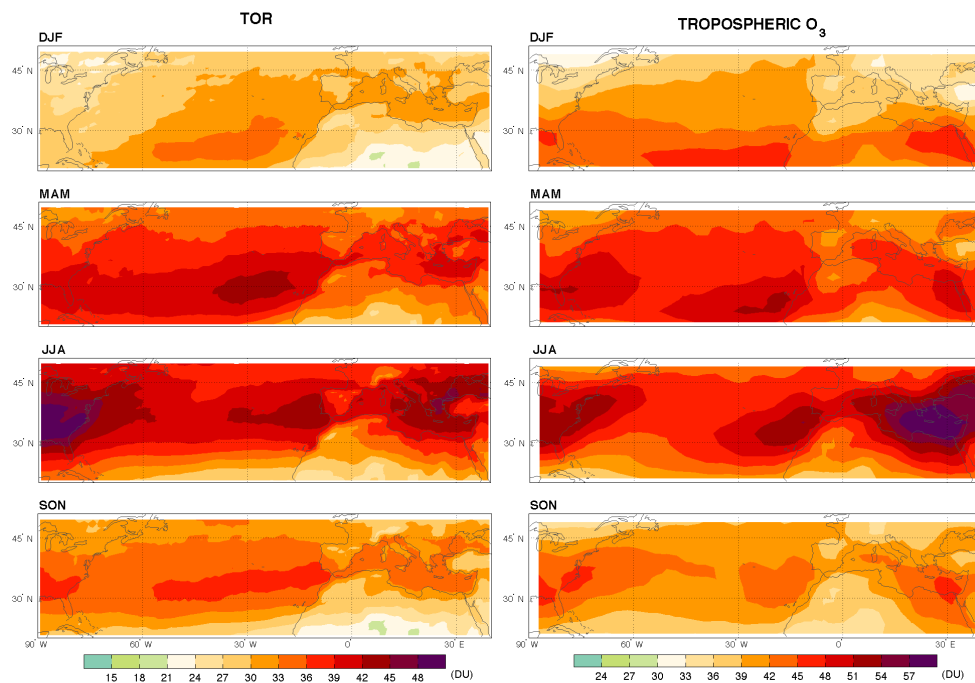


**Fig. 3.** Climatological (1980–2005) tropospheric ozone residual (left) and modeled tropospheric  $O_3$  burden (right) in the North Atlantic for each season. Note the use of different colorscales to better visualize similarities in the patterns.

## Model analysis and measurements intercomparison

F. S. R. Pausata et al.

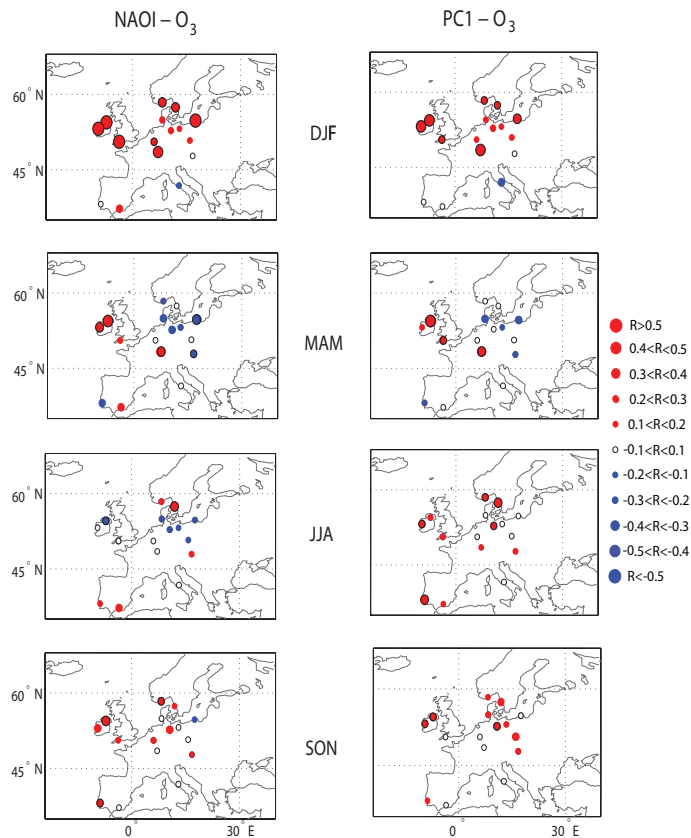


**Fig. 4.** Seasonal correlation between NAOI (left) and PC1 (right), and surface  $O_3$  concentrations measured by the ground stations listed in Table 1. The correlation intervals are shown in the legend. Black bold rings indicate significant correlation with 90 % confidence.

## Model analysis and measurements intercomparison

F. S. R. Pausata et al.

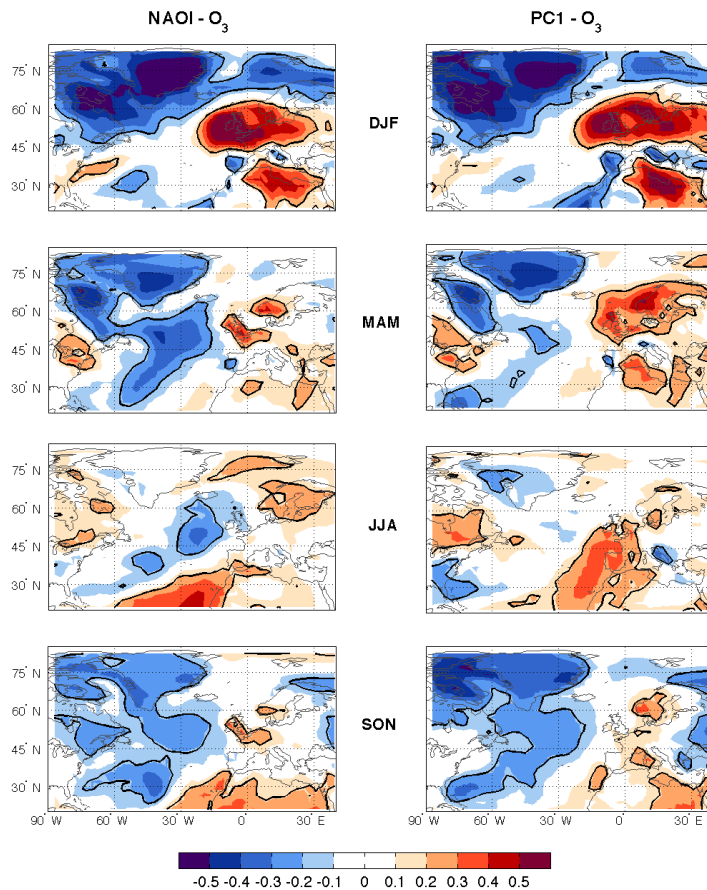


**Fig. 5.** Correlation between NAOI (left) and PC1 (right), and surface  $O_3$  concentrations for each season. The contours indicate where the correlation is significant with 90 % confidence.

[Title Page](#)
[Abstract](#)
[Introduction](#)
[Conclusions](#)
[References](#)
[Tables](#)
[Figures](#)
[Back](#)
[Close](#)
[Full Screen / Esc](#)
[Printer-friendly Version](#)
[Interactive Discussion](#)

Model analysis and  
measurements  
intercomparison

F. S. R. Pausata et al.

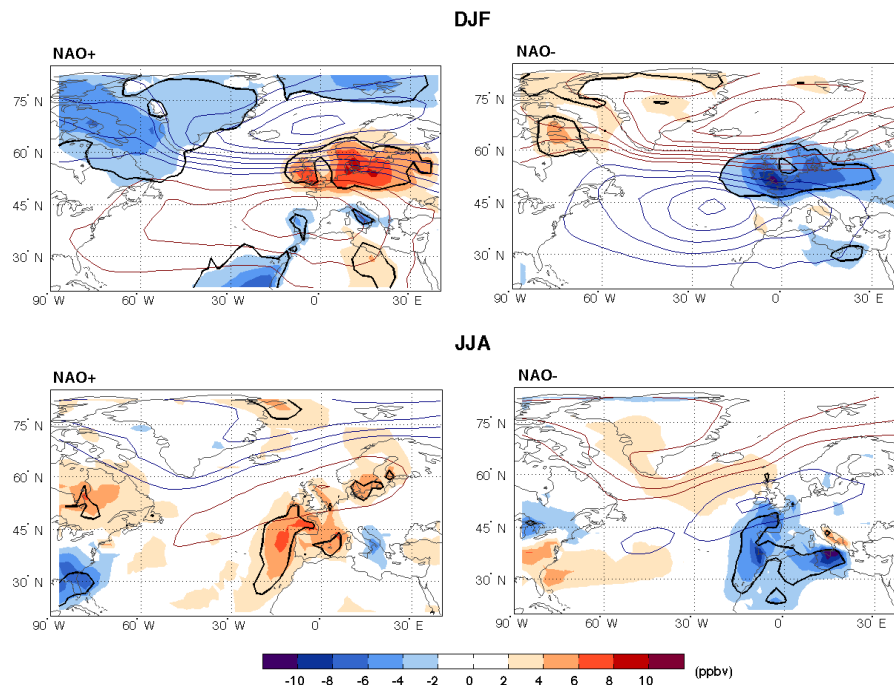


**Fig. 6.** Positive (red contours) and negative (blue contours) SLP and surface  $O_3$  concentration (color shading) anomalies associated with the ensemble average of positive (right) and negative (left) NAO phase winter (top) and summer (bottom) months. Contours have 1.5 hPa interval. The bold black contours indicates  $O_3$  anomalies greater than 0.5 standard deviation.

Title Page

Abstract

Introduction

Conclusions

References

Tables

Figures

◀

▶

◀

▶

Back

Close

Full Screen / Esc

Printer-friendly Version

Interactive Discussion



**Model analysis and measurements intercomparison**

F. S. R. Pausata et al.

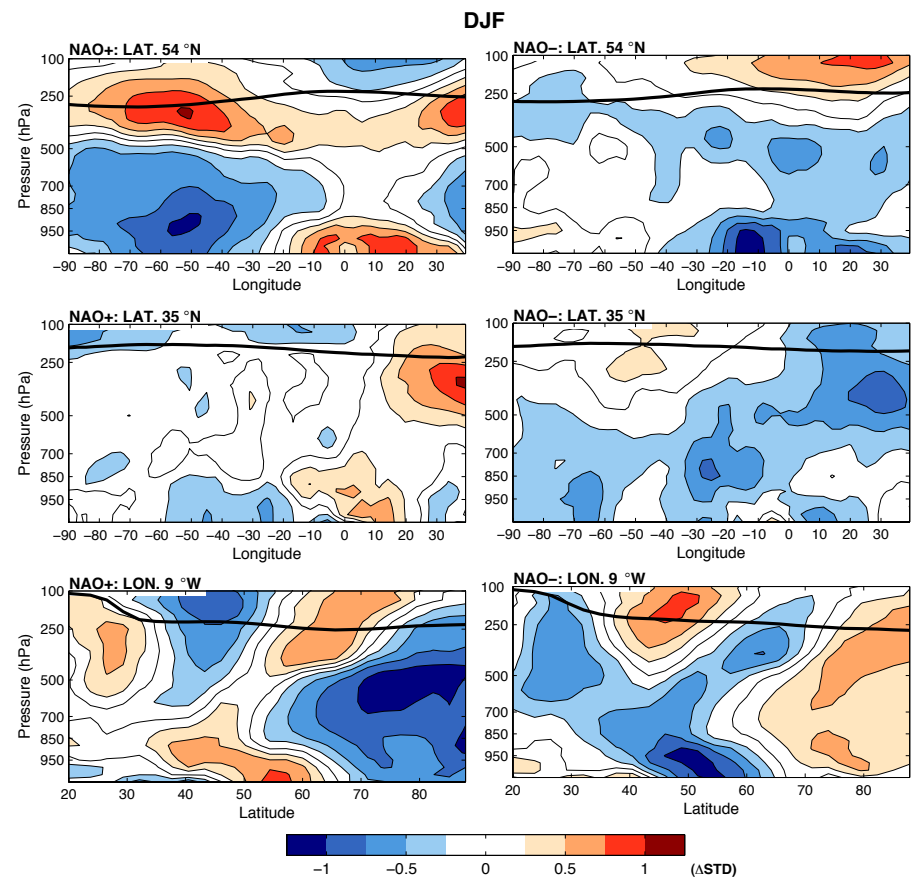


**Fig. 7.** Transect of normalized O<sub>3</sub> concentration anomalies for a given latitude (upper and middle panels) and longitude (lower panels) as a function of pressure in winter. O<sub>3</sub> concentration anomalies are normalized by O<sub>3</sub> standard deviation. Thick solid line indicates the tropopause height.

Title Page

Abstract   Introduction

Conclusions   References

Tables   Figures

◀   ▶

◀   ▶

Back   Close

Full Screen / Esc

Printer-friendly Version

Interactive Discussion



Model analysis and  
measurements  
intercomparison

F. S. R. Pausata et al.

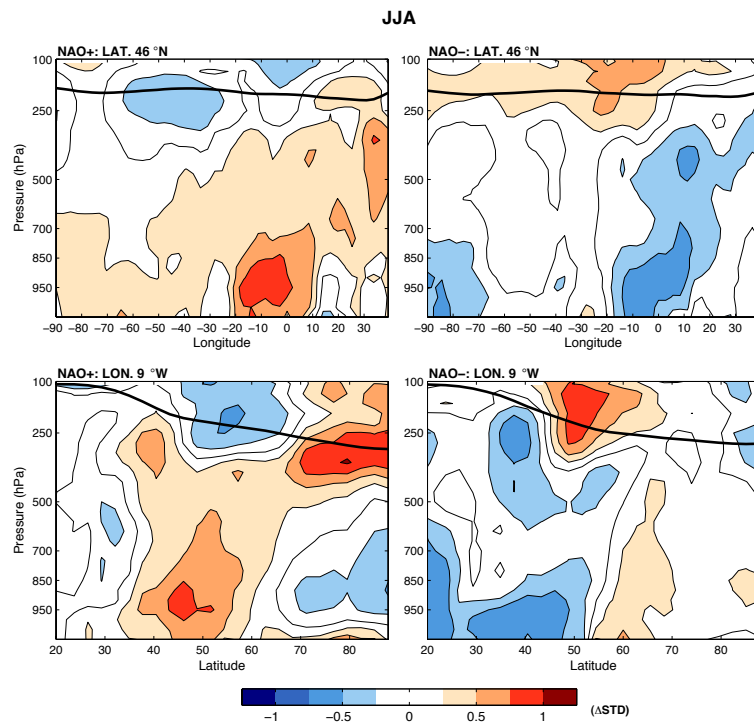


**Fig. 8.** Transect of normalized  $O_3$  concentration anomalies for a given latitude (upper panels) and longitude (lower panels) as a function of pressure in summer.  $O_3$  concentration anomalies are normalized by  $O_3$  standard deviation. Thick solid line indicates the tropopause height.

Title Page

Abstract

Introduction

Conclusions

References

Tables

Figures

◀

▶

◀

▶

Back

Close

Full Screen / Esc

Printer-friendly Version

Interactive Discussion



**Model analysis and  
measurements  
intercomparison**

F. S. R. Pausata et al.

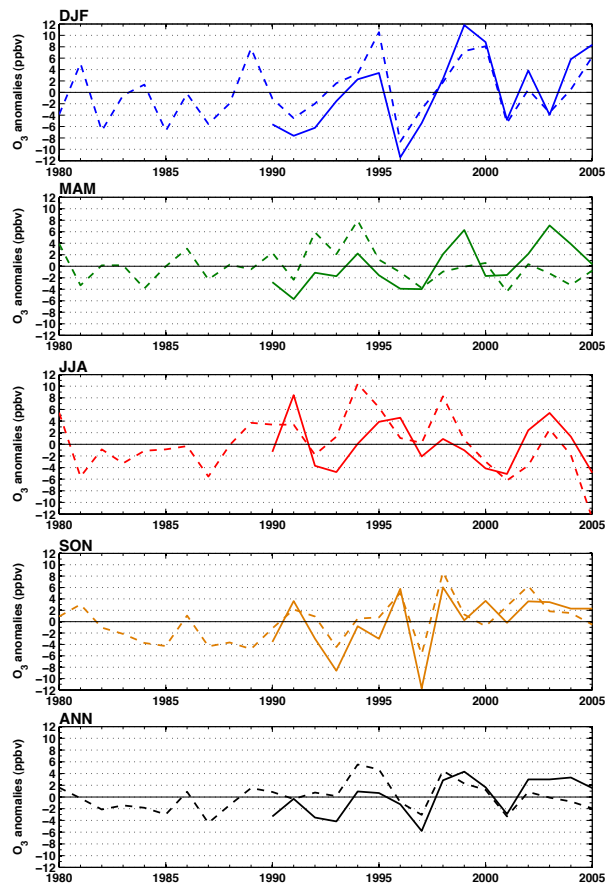


**Fig. 9.** Modelled (dashed lines) and observed (solid lines) surface O<sub>3</sub> concentration trends at Mace Head for each season and the annual mean.

Title Page

Abstract

Introduction

Conclusions

References

Tables

Figures

◀

▶

◀

▶

Back

Close

Full Screen / Esc

Printer-friendly Version

Interactive Discussion

